Maximum-Throughput Irregular Distributed Space-Time Code for Near-Capacity Cooperative Communications

Lingkun Kong, Soon Xin Ng, Robert G. Maunder, and Lajos Hanzo

***Abstract*— This paper presents an Irregular Distributed Space-Time (Ir-DST) coding scheme designed for near-capacity cooperative communications where the system's effective throughput is also maximized with the aid of a joint source-and-relay mode design procedure. At the source node, a serial concatenated scheme comprising an IRregular Convolutional Code (IRCC), a recursive Unity-Rate Code (URC) and a Space-Time Block Code (STBC) was designed for the sake of approaching the corresponding source-to-relay link capacity, where the IRCC was optimized with the aid of EXtrinsic Information Transfer (EXIT) charts. At the relay node, another IRCC is concatenated serially with an identical STBC. Before transmitting the relayed information, the relay's IRCC is re-optimized based on EXIT chart analysis for the sake of approaching the relay channel's capacity as well as for maximizing the relay's coding rate, which results in a maximized effective throughput. We will demonstrate that the topology of the Ir-DST system coincides with that of a Distributed Turbo Code (DTC). At the destination node, a novel three-stage iterative decoding scheme is constructed in order to achieve decoding convergence to an infinitesimally low Bit Error Ratio (BER). Finally, our numerical results show the proficiency of our joint source-and-relay mode design procedure, demonstrating that the proposed Ir-DST coding scheme is capable of near-capacity cooperative communications as well as of maximizing the effective throughput.**

***Index Terms*— Irregular distributed space-time code, iterative detection, EXIT charts.**

I. Introduction

In the past few years, cooperative communication schemes [1]–[3] have been intensively studied, which combine the benefits of distributed Multiple-Input Multiple-Output (MIMO) systems with relay technologies. In a relay network, where the nodes (users) are equipped with either single or multiple antennas, cooperative communications allow the nodes (users) to assist each other in forwarding (relay) all messages to the destination, rather than transmitting only their own messages. Since the MIMO transmitter's elements in such a network are distributed, the network forms a "distributed MIMO" system. For the sake of improving the diversity gain of relay-aided networks, numerous cooperative protocols [1]–[4] have been proposed. In most cooperative scenarios, predominantly the Decode-and-Forward (DF) and Amplify-and-Forward (AF) protocols are used. However, a strong channel code is required for mitigating the potential error propagation in the DF scheme or to avoid the noise-enhancement in the AF scheme.

Inspired by the classic turbo codes used in non-cooperative communication scenarios, Distributed Turbo Codes (DTC) [5] have been proposed for "distributed MIMO" systems, which benefit from a *turbo processing* gain. However, DTCs suffer from having an imperfect communication link between the source and relay nodes. Hence a three-component Distributed Turbo Trellis Coded Modulation (DTTCM) scheme has been proposed in [6], which takes into consideration the realistic condition of having an imperfect source-to-relay communication link. The DTTCM scheme [6] designed using EXtrinsic Information Transfer (EXIT) chart analysis [7], [8] is capable of minimizing the decoding error probability at the relay node and performs close to its idealized counterpart that assumes perfect decoding at the relay node. However, the DTTCM of [6] still fails to approach the corresponding relay channel's capacity.

On the other hand, there exist several capacity-approaching turbo coding schemes designed for specific network topologies proposed in [9] by Zhang and Duman for half-duplex relay systems, where the authors did not aim for proposing a general design procedure to find the optimal coding schemes under different relay network configurations. Against this background, our objective here is to design a near-capacity cooperative scheme using a joint source-and-relay mode design procedure, which is suitable for arbitrary relay network configurations. Furthermore, the relay system's effective throughput is maximized as a benefit of the proposed design procedure. For the sake of approaching the relay channel's capacity, we first derive the theoretical lower and upper bounds on the Continuous-input Continuous-output Memoryless Channel's (CCMC) [10], [11] capacity as well as of the Discrete-input Continuous-output Memoryless Channel (DCMC) [10], [11] capacity (constrained information rate) with independent and uniformly distributed (i.u.d) inputs. A new Irregular Distributed Space-Time (Ir-DST) coding scheme is proposed, where two IRregular Convolutional Codes (IRCC) [12], [13] having different IRCC weighting coefficients are employed at the source and relay nodes, respectively, which are designed for supporting near-capacity cooperative communications.

The rest of this paper is organised as follows. The system model is described in Section II. Section III specifies the encoding and decoding processes of the novel Ir-DST coding scheme. The relay channel's capacity computation and the EXIT chart aided joint source-and-relay mode design are detailed in Section IV, while our simulation results and discussions are provided in Section V. Finally, we conclude

The authors are with School of Electronics and Computer Science, University of Southampton, SO17 1BJ, United Kingdom. Email: {lk06r,sxn,rm,lh}@ecs.soton.ac.uk.

The financial support of the China-UK Scholarship Council, as well as that of the EPSRC UK, the EU under the auspices of the Optimix project is gratefully acknowledged.

in Section VI.

II. System Model

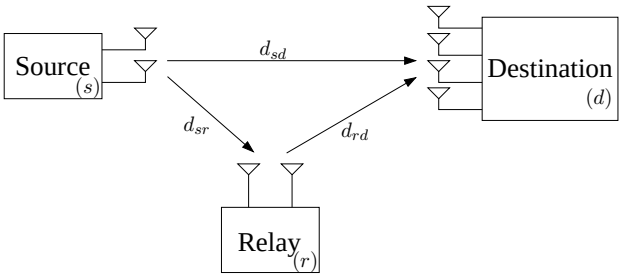

Fig. 1. Schematic of a single relay aided multi-antenna system, where d_{ab} is the geographical distance between node *a* and node *b*.

We consider a two-hop relay-aided network, which has a single source node having N_s antennas, a single relay node equipped with N_r antennas and a destination node having N_d antennas, where all nodes obey the half-duplex constraint, i.e. a node cannot transmit and receive simultaneously. The schematic of the proposed system is shown in Fig. 1, which typically entails two phases. In *Phase I*, the source node (s) broadcasts the information both to the relay node (r) and to the destination node (d). The relay node (r) processes the received information and forwards it to the destination node (d) in *Phase II*, while the source node (s) remains silent. The destination performs decoding based on the messages it received in both phases. As in [14], we model the communication links in Fig. 1 as being subjected to both long-term free-space path loss as well as to short-term uncorrelated Rayleigh fading.

Let d_{ab} and P_{ab} denote the geometrical distance and the path loss between nodes *a* and *b*. The path loss and the geometrical distance can be related by [14]

$$P_{ab} = \frac{K}{d_{ab}^{\alpha}}, \tag{1}$$

where K is a constant that depends on the environment and α is the path-loss exponent. For a free space scenario, we have $\alpha = 2$. The relationship between the energy E_{sr} received at the relay node and that of the destination node E_{sd} can be expressed as

$$E_{sr} = \frac{P_{sr}}{P_{sd}} E_{sd} = G_{sr} E_{sd}, \tag{2}$$

where G_{sr} is the power-gain (or geometrical-gain) [14] experienced by the source-to-relay link with respect to the source-to-destination link as a benefit of the commensurately reduced distance and path loss, which can be expressed as

$$G_{sr} = \left(\frac{d_{sd}}{d_{sr}}\right)^2. \tag{3}$$

Similarly, the geometrical-gain at the relay-to-destination link with respect to the source-to-destination link can be formulated as

$$G_{rd} = \left(\frac{d_{sd}}{d_{rd}}\right)^2. \tag{4}$$

Naturally, the geometrical-gain at the source-to-destination link with respect to itself is unity, i.e. $G_{sd} = 1$. Therefore, owing to the triangle inequality applied in Fig. 1, the geometrical-gains G_{sr} and G_{rd} have to satisfy

$$G_{sr} + G_{rd} + 2\sqrt{G_{sr} G_{rd}} \geq G_{sr} G_{rd}. \tag{5}$$

We assume that the relay node is closer to the source node than to the destination node, while both the source and relay are far away from the destination, namely we have $G_{sr} > G_{rd}$. In this scenario, the relay benefits from a higher received signal power than the destination. This assumption facilitates the employment of near-perfect DF relaying (similar arguments can be found in [15], [16]), otherwise other relaying modes might be better choices (e.g. Amplify-and-Forward (AF) and Compress-and-Forward (CF)). Hence, the vector hosting the received signal at the relay node during *Phase I*, which consists of L_s number of symbol periods, can be formulated as

$$\mathbf{y}_r = \sqrt{G_{sr}} \mathbf{H}_{sr} \mathbf{c}_s + \mathbf{n}_r, \tag{6}$$

where $\mathbf{y}_r = [y_{r,1}, \ldots, y_{r,N_r}]^T$ is the N_r-element vector of the received signals at the relay node, $\mathbf{H}_{sr}$ is the $(N_r \times N_s)$-element channel matrix, the entries of which are independent and identically complex Gaussian distributed with a zero mean and a variance of 0.5 per dimension. Furthermore, $\mathbf{c}_s = [c_{s,1}, \ldots, c_{s,N_s}]^T$ is an N_s-element vector of the signals transmitted from the source node at an average power of P_0 and $\mathbf{n}_r = [n_{r,1}, \ldots, n_{r,N_r}]^T$ is an N_r-element noise vector. Each element of $\mathbf{n}_r$ is an Additive White Gaussian Noise (AWGN) process having a zero mean and a variance of $N_0/2$ per dimension. By contrast, the signal vector received at the destination node during *Phase I* can be expressed as

$$\mathbf{y}_d^I = \sqrt{G_{sd}} \mathbf{H}_{sd} \mathbf{c}_s + \mathbf{n}_d, \tag{7}$$

and the signal vector received at the destination node during *Phase II*, when L_r number of symbols are transmitted from the relay node, is formulated as

$$\mathbf{y}_d^{II} = \sqrt{G_{rd}} \mathbf{H}_{rd} \mathbf{c}_r + \mathbf{n}_d, \tag{8}$$

where $\mathbf{y}_d^I = [y_{d,1}^I, \ldots, y_{d,N_d}^I]^T$ and $\mathbf{y}_d^{II} = [y_{d,1}^{II}, \ldots, y_{d,N_d}^{II}]^T$ are both N_d-element vectors of the signals received during *Phase I* and *Phase II* at the destination node, $\mathbf{H}_{sd} \in \mathbb{C}^{N_d \times N_s}$ and $\mathbf{H}_{rd} \in \mathbb{C}^{N_d \times N_r}$ are the corresponding channel matrices, the entries of which are independent and identically complex Gaussian distributed with a zero mean and a variance of 0.5 per dimension. Finally, $\mathbf{c}_r = [c_{r,1}, \ldots, c_{r,N_r}]^T$ is an N_r-element vector of the signals transmitted from the relay node at the same power P_0 as that of $\mathbf{c}_s$ and $\mathbf{n}_d = [n_{d,1}, \ldots, n_{d,N_d}]^T$ is an N_d-element AWGN vector with each element having a zero mean and a variance of $N_0/2$ per dimension.

III. Irregular Distributed Space-Time Codes

A. Ir-DST Encoder

In this contribution, we consider a specific two-hop relay-aided network associated with $N_s = 2$, $N_r = 2$ and $N_d = 4$, as shown in Fig. 1. At the source node, we use Alamouti's STBC [17] amalgamated with a recursive Unity-Rate

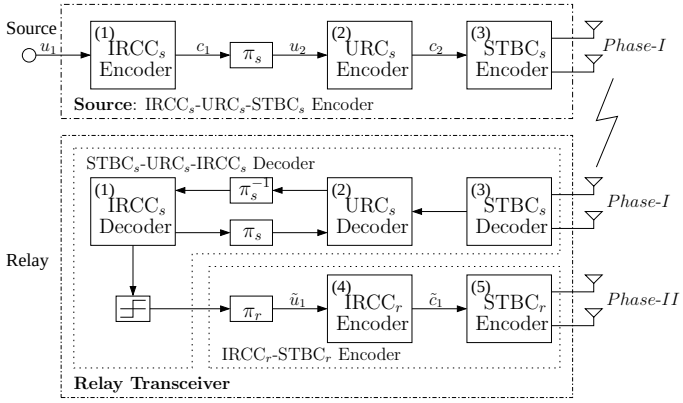

Fig. 2. Schematic of the Irregular Distributed Space-Time (Ir-DST) encoder.

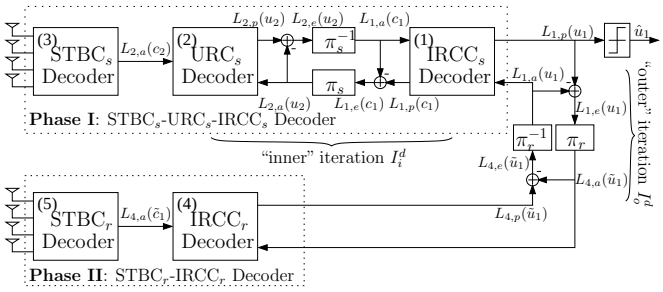

Fig. 3. The three-stage iterative decoder of the Irregular Distributed Space-Time (Ir-DST) coding scheme.

Code (URC)[1] used as the inner code, while an IRCC [12], [13] having an average code rate of R_s is employed as the outer code, which is optimized with the aid of EXIT chart analysis for the sake of near-error-free decoding at channel SNRs close to the capacity of the source-to-relay link at the relay node during the relay's receive period of *Phase I*. On the other hand, as shown in Fig. 2, in the relay's transmit period of *Phase II* another IRCC having a code rate of R_r is amalgamated with Alamouti's STBC scheme, where the IRCC is further improved with the aid of a joint source-and-relay mode design procedure, as we will show in Section IV-B for the sake of approaching the relay channel's capacity. Specifically, the notations π_s and π_r in Fig. 2 represent the bit-wise random interleaver used at the source node and the relay node, respectively. Compared to the topology of the DTC [5], it may be observed that the cooperative scheme seen in Fig. 2 combines the benefits of a serially concatenated scheme and of a DTC, which is referred to as an Irregular Distributed Space-Time (Ir-DST) coding scheme in this contribution.

B. Three-Stage Iterative Decoding at the Destination

The novel three-stage iterative decoder structure of the Ir-DST scheme is illustrated in Fig. 3. At the destination node, the signals received during *Phase I* are first decoded by the amalgamated[2] "STBC$_s$-URC$_s$" decoder in order to produce the *a priori* Log-Likelihood Ratio (LLR) values $L_{1,a}(c_1)$ of the coded bits c_1 by the Maximum Aposteriori Probability (MAP) algorithm [19]. The IRCC$_s$ decoder seen at the top right of Fig. 3 processes the information forwarded by the "STBC$_s$-URC$_s$" decoder in conjunction with the *a priori* LLR values $L_{1,a}(u_1)$ of the information bits u_1 gleaned by the "STBC$_r$-IRCC$_r$" relay-decoder in order to generate the *a posteriori* LLR values $L_{1,p}(u_1)$ and $L_{1,p}(c_1)$ of the information bits u_1 and of the coded bits c_1, respectively. As seen in Fig. 3, the *a priori* LLRs $L_{1,a}(c_1)$ are subtracted from the *a posteriori* LLR values $L_{1,p}(c_1)$ and then they are fed back to the "STBC$_s$-URC$_s$" decoder as the *a priori* information $L_{2,a}(u_2)$ through the interleaver π_s. We term this information-exchange process seen in the top trace of Fig. 3 as the "inner" iteration[3]. Similarly, during the "outer" iterations, the *a priori* LLR values $L_{1,a}(u_1)$ fed into the IRCC$_s$ decoder are also subtracted from the *a posteriori* LLR values $L_{1,p}(u_1)$ for the sake of generating the extrinsic LLR values $L_{1,e}(u_1)$ as seen at the top right corner of Fig. 3. Then $L_{1,e}(u_1)$ is passed to the amalgamated "STBC$_r$-IRCC$_r$" relay-decoder as the *a priori* information $L_{4,a}(\tilde{u}_1)$ through the interleaver π_r in conjunction with the signals received during *Phase II* in order to compute the *a posteriori* LLR values $L_{4,p}(\tilde{u}_1)$ of the permuted information bits $\tilde{u}_1$ from the relay node. As seen in Fig. 3, the extrinsic information $L_{4,e}(\tilde{u}_1)$ is generated by subtracting the *a priori* information $L_{4,a}(\tilde{u}_1)$ from the *a posteriori* information $L_{4,p}(\tilde{u}_1)$, before $L_{4,e}(\tilde{u}_1)$ is fed back to the IRCC$_s$ decoder as the *a priori* information $L_{1,a}(u_1)$ through the de-interleaver π_r^{-1}. During the last "outer" iteration, only the LLR values $L_{1,p}(u_1)$ of the original information bits u_1 are required, which are passed to the hard-decision block of Fig. 3 in order to estimate the source bits.

IV. Near-Capacity System Design and Analysis

In order to design a near-capacity coding scheme for the proposed two-hop relay-aided network, in Section IV-A we first derive the upper and lower bounds on the relay channel's CCMC capacity as well as those of the DCMC capacity (constrained information rate) for Alamouti's STBC scheme, since the relay channel's exact capacity formula is unavailable. Then, the EXIT chart based joint source-and-relay mode design will be carried out in Section IV-B.

A. Relay Channel's Capacity

As presented in [15], a general upper bound on the CCMC capacity of a half-duplex[4] relay system may be derived based on the original results of [20] on the full-duplex relay channels,

[1]URCs were proposed by Divsalar *et al.* [18] for the sake of extending the overall system's impulse response to an infinite duration, which efficiently spreads the extrinsic information, hence improves the achievable iterative detection gain.

[2]The terminology "amalgamated" is used here to indicate that although it might have some benefits to exchange extrinsic information between these two blocks, no iterations were used between them.

[3]Explicitly, at the destination node, the extrinsic information exchange between the amalgamated "STBC$_s$-URC$_s$" decoder and the IRCC$_s$ decoder is referred to as the "inner" iteration, while that between the parallel amalgamated "STBC$_s$-URC$_s$-IRCC$_s$" decoder and the amalgamated "STBC$_r$-IRCC$_r$" relay-decoder is referred to as the "outer" iteration.

[4]In [15], the source node continues transmission during the second time slot.

which is given by

$$C_{\text{CCMC}}^{\text{coop}} \leq \max_{p(x_1,x_2,x)} \min\{\lambda E\left[I(X_1;Y_1,Y)\right]+(1-\lambda)E\left[I(X_2;Y_2|X)\right], \lambda E\left[I(X_1;Y_1)\right]+(1-\lambda)E\left[I(X_2,X;Y_2)\right]\}. \quad (9)$$

where λ is the ratio of the first time slot duration to the total frame duration. On the other hand, another achievable rate definition for the DF protocol, which can be regarded as a lower bound on the CCMC capacity of the relay system, was provided in [15] in the form of

$$C_{\text{CCMC}}^{\text{coop}} \geq \max_{p(x_1,x_2,x)} \min\{\lambda E\left[I(X_1;Y)\right]+(1-\lambda)E\left[I(X_2;Y_2|X)\right], \lambda E\left[I(X_1;Y_1)\right]+(1-\lambda)E\left[I(X_2,X;Y_2)\right]\}, \quad (10)$$

where $p(x_1,x_2,x)$ indicates the joint probability of the signals transmitted from the source and the relay nodes. The signals X_1 and X_2 are transmitted from the source node during the first and the second time slot, respectively, while Y_1 and Y_2 represent the corresponding signals received at the destination during the two consecutive time slots. Furthermore, X and Y are the transmitted and received signals at the relay node, respectively.

In our half-duplex-constrained relay-aided system, the source node does not transmit during *Phase II*, i.e. $X_2 = 0$, we have $E[I(X_2;Y_2|X)] = 0$ and $E[I(X_2,X;Y_2)] = E[I(X;Y_2)]$ in (9) and (10). Hence, based on Eqs. (6)-(8) the upper and lower bounds of the relay channel's capacity can be derived accordingly as

$$C_{\text{CCMC}}^{\text{coop}} \leq \max_{p(c_s,c_r)} \min\{\frac{L_s}{L_s+L_r}E\left[I(C_s;Y_d^I,Y_r)\right], \frac{L_s}{L_s+L_r}E\left[I(C_s;Y_d^I)\right]+\frac{L_r}{L_s+L_r}E\left[I(C_r;Y_d^{II})\right]\} \quad (11)$$

and

$$C_{\text{CCMC}}^{\text{coop}} \geq \max_{p(c_s,c_r)} \min\{\frac{L_s}{L_s+L_r}E\left[I(C_s;Y_r)\right], \frac{L_s}{L_s+L_r}E\left[I(C_s;Y_d^I)\right]+\frac{L_r}{L_s+L_r}E\left[I(C_r;Y_d^{II})\right]\}, \quad (12)$$

respectively.

In addition to the CCMC capacity bounds of (11) and (12), we evaluate the information-rate bounds for the relaying channel in conjunction with i.u.d inputs. In this contribution, we employ Alamouti's G2 scheme [17] at both the source and relay nodes, whose *codeword* matrix is given by

$$\mathbf{C}_{G2} = \begin{pmatrix} c_1 & c_2 \\ -c_2^* & c_1^* \end{pmatrix}^T. \quad (13)$$

Based on Eqs. (6)-(8), the signal received at the relay node during $V = 2$ consecutive symbol periods can be written as

$$\mathbf{Y}_r = \sqrt{G_{sr}}\mathbf{H}_{sr}\mathbf{C}_s + \mathbf{N}_r, \quad (14)$$

while the signals received at the destination node during $V = 2$ consecutive symbol periods in *Phase I* and *Phase II* are expressed as

$$\mathbf{Y}_d^I = \sqrt{G_{sd}}\mathbf{H}_{sd}\mathbf{C}_s + \mathbf{N}_d, \quad (15)$$

and

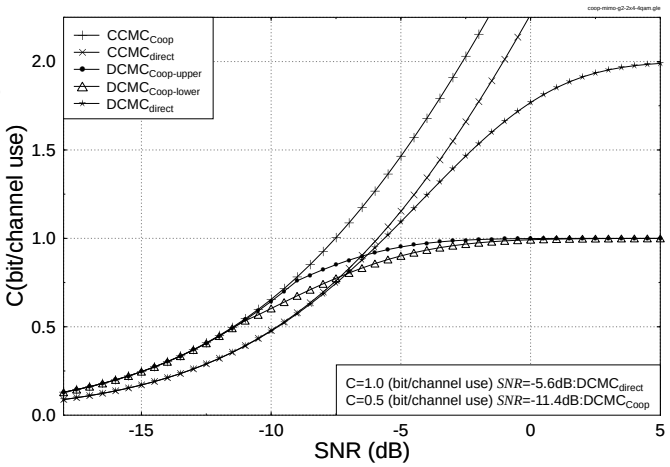

Fig. 4. The relay channel's CCMC capacity and constrained information-rate bounds employing the 4QAM-modulated G2 scheme when the network is configured with $G_{sr} = 8$ and $G_{rd} = 2$ as well as $L_s = L_r$.

$$\mathbf{Y}_d^{II} = \sqrt{G_{rd}}\mathbf{H}_{rd}\mathbf{C}_r + \mathbf{N}_d, \quad (16)$$

respectively. Specifically, $\mathbf{Y}_r = [\mathbf{y}_{r,1},\ldots,\mathbf{y}_{r,V}] \in \mathbb{C}^{N_r\times V}$, $\mathbf{Y}_d^I = [\mathbf{y}_{d,1}^I,\ldots,\mathbf{y}_{d,V}^I] \in \mathbb{C}^{N_d\times V}$ and $\mathbf{Y}_d^{II} = [\mathbf{y}_{d,1}^{II},\ldots,\mathbf{y}_{d,V}^{II}] \in \mathbb{C}^{N_d\times V}$ are the matrices hosting the sampled signal received at the relay node and the destination node, respectively, while $\mathbf{H}_{sr} \in \mathbb{C}^{N_r\times N_s}$, $\mathbf{H}_{sd} \in \mathbb{C}^{N_d\times N_s}$ and $\mathbf{H}_{rd} \in \mathbb{C}^{N_d\times N_r}$ are the corresponding quasi-static channel matrices, which are constant over $V = 2$ consecutive symbol periods. Furthermore, $\mathbf{C}_s = [\mathbf{c}_{s,1},\ldots,\mathbf{c}_{s,V}] \in \mathbb{C}^{N_s\times V}$ and $\mathbf{C}_r = [\mathbf{c}_{r,1},\ldots,\mathbf{c}_{r,V}] \in \mathbb{C}^{N_r\times V}$ represent Alamouti's G2 matrices characterizing the transmissions of the source and relay nodes, while $\mathbf{N}_r = [\mathbf{n}_{r,1},\ldots,\mathbf{n}_{r,V}] \in \mathbb{C}^{N_r\times V}$ and $\mathbf{N}_d = [\mathbf{n}_{d,1},\ldots,\mathbf{n}_{d,V}] \in \mathbb{C}^{N_d\times V}$ represents the AWGN matrix incurred at the relay and the destination nodes, respectively.

Hence, we may readily derive the upper and lower bounds on the constrained information rate of the relaying channel with i.u.d G2 *codeword*-matrix inputs as

$$C_{\text{DCMC}}^{\text{coop-g2}} \leq \min\{\frac{L_s}{L_s+L_r}E\left[I(\mathbf{C}_s;\mathbf{Y}_d^I,\mathbf{Y}_r)\right], \frac{L_s}{L_s+L_r}E\left[I(\mathbf{C}_s;\mathbf{Y}_d^I)\right]+\frac{L_r}{L_s+L_r}E\left[I(\mathbf{C}_r;\mathbf{Y}_d^{II})\right]\} \quad (17)$$

and

$$C_{\text{DCMC}}^{\text{coop-g2}} \geq \min\{\frac{L_s}{L_s+L_r}E\left[I(\mathbf{C}_s;\mathbf{Y}_r)\right], \frac{L_s}{L_s+L_r}E\left[I(\mathbf{C}_s;\mathbf{Y}_d^I)\right]+\frac{L_r}{L_s+L_r}E\left[I(\mathbf{C}_r;\mathbf{Y}_d^{II})\right]\}, \quad (18)$$

respectively, where the corresponding constrained information rates of $E\left[I(\mathbf{C}_s;\mathbf{Y}_d^I,\mathbf{Y}_r)\right]$, $E\left[I(\mathbf{C}_s;\mathbf{Y}_r)\right]$, $E\left[I(\mathbf{C}_s;\mathbf{Y}_d^I)\right]$ and $E\left[I(\mathbf{C}_r;\mathbf{Y}_d^{II})\right]$ can be computed based on Eq. (9) of [21].

An example for a specific network configuration associated with $L_s = L_r$ as well as $G_{sr} = 8$ and $G_{rd} = 2$ is given in Fig. 4, where the direct transmission based benchmarker is also depicted with the power constraint P_0 for a fair comparison. The CCMC capacity and the information rates obeying the i.u.d 4QAM-modulated G2 *codeword*-matrix-input constraint are evaluated by the upper and lower bounds given in (11)-(12) and (17)-(18). We can see in Fig. 4 that the lower and

upper bounds converge and exhibit a substantial capacity gain over conventional direct transmission in the low and medium SNR regimes below a certain convergence threshold, which is caused by the geometrical-gain of the relay-to-destination link. On the other hand, it is observed that the relay channel's DCMC capacity is only half of the direct transmission due to a factor of $\frac{L_r}{L_s+L_r} = 0.5$ multiplexing loss in the half-duplex scenario. The DCMC capacity provides the fundamental limits on the performance of a practical coding/decoding scheme. In Section IV-B, we will propose an optimal distributed coding scheme, which is capable of approaching the relay channel's limits under arbitrary relay network configuration.

B. Joint Code Design for the Source-and-Relay Nodes Based on EXIT Charts

For the sake of analysing the convergence behaviours of iterative decoders employed by the two-hop relay-aided system, we use two EXIT charts [7], [8] to examine the evolution of the input/output mutual information exchanges between the inner amalgamated "STBC$_s$-URC$_s$" decoder and the outer IRCC$_s$ decoder at the relay node, as well as between the parallel amalgamated "STBC$_s$-URC$_s$-IRCC$_s$" decoder and the amalgamated "STBC$_r$-IRCC$_r$" decoder at the destination node during the consecutive iterations. As has been investigated in [22], [23], a narrow but marginally open EXIT-tunnel between the EXIT curves of the inner amalgamated "STBC$_s$-URC$_s$" decoder and the outer IRCC$_s$ decoder at the relay node indicates that a performance close to the capacity of the source-to-relay link could be achieved. Similarly, at the destination node, a narrow-but-open EXIT-tunnel between the EXIT curves of the parallel amalgamated "STBC$_s$-URC$_s$-IRCC$_s$" decoder and the amalgamated "STBC$_r$-IRCC$_r$" decoder indicates the possibility of achieving decoding convergence to an infinitesimally low Bit Error Ratio (BER) at SNRs close to the relay channel's capacity. Therefore, we propose a joint source-and-relay mode design procedure for supporting near-capacity cooperative communications as well as for maximizing the system's effective throughput, which can be simplified to two EXIT curve matching problems summarised as follows:

Step 1: Choose a specific average code rate R_s for the IRCC$_s$ at the source node and employ the EXIT curve matching algorithm of [12] to obtain the optimized weighting coefficients $\alpha_i, i = 1,\ldots,17$ of IRCC$_s$, where a narrow but marginally open EXIT-tunnel between the EXIT curves of the inner amalgamated "STBC$_s$-URC$_s$" decoder and the outer IRCC$_s$ decoder emerges at the relay node. This implies that a near-capacity performance may be achieved for the source-to-relay communication link. Then we store the value of the corresponding transmit power required at the source node.

Step 2: Choose the same transmit power at the source as stored in **Step 1**. Fix the optimized weighting coefficients $\alpha_i, i = 1,\ldots,17$ of the IRCC$_s$ obtained in **Step 1** at the source node, perform iterative decoding by exchanging extrinsic information between the amalgamated "STBC$_s$-URC$_s$" decoder and the IRCC$_s$ decoder during *Phase I* at the destination node, until the further increase of the area A_E under the EXIT curve of the amalgamated "STBC$_s$-URC$_s$-IRCC$_s$" decoder becomes marginal, then stop this "inner" iterative decoding process.

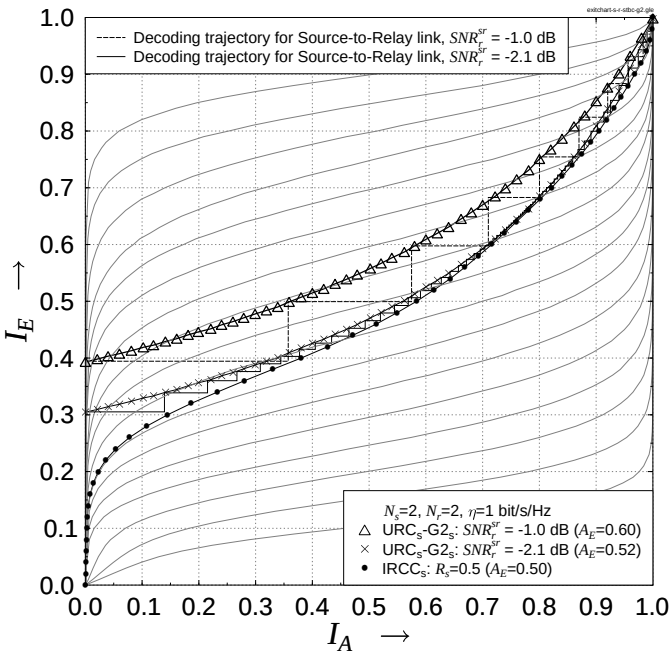

Fig. 5. The EXIT chart curves of the URC$_s$-G2$_s$, the IRCC$_s$ with optimized weighting coefficients $[\alpha_1,\ldots,\alpha_{17}]$= [0, 0, 0, 0, 0, 0.327442, 0.186505, 0.113412, 0, 0.0885527, 0, 0.0781214, 0.0962527, 0.0114205, 0.0346015, 0.0136955, 0.0500168] and 17 IRCC subcodes for the 2×2 source-to-relay communication link.

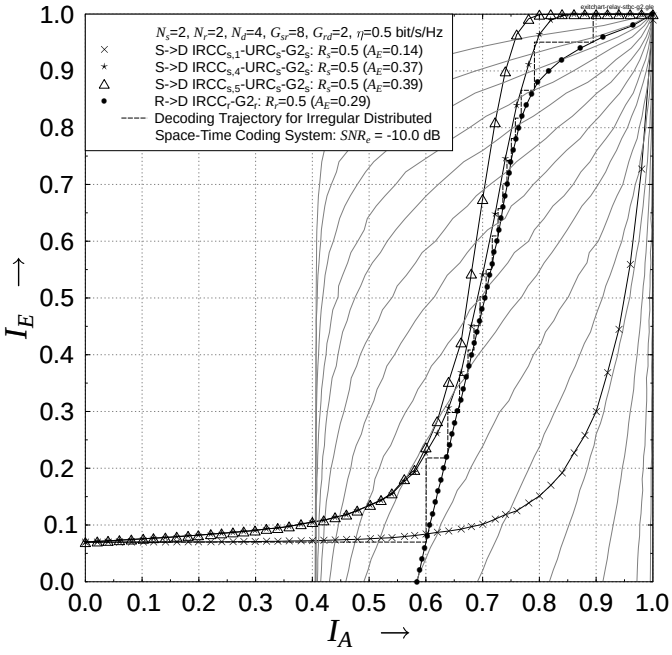

Fig. 6. The EXIT chart curves for the IRCC$_s$-URC$_s$-G2$_s$ with various "inner" iterations, the IRCC$_r$-G2$_r$ with IRCC$_r$ having optimized weighting coefficients $[\beta_1,\ldots,\beta_{17}]$ = [0, 0, 0, 0, 0.233115, 0.0158742, 0.292084, 0.220065, 0.0151108, 0, 0, 0, 0, 0, 0, 0, 0.22375] and 17 SNR-dependent IRCC$_r$-G2$_r$ subcodes. The subscript of IRCC$_s$ denotes the number of "inner" iterations between the IRCC$_s$ and "G2$_s$-URC$_s$" decoders and the SNR$_e$ represents the equivalent SNR at both the source and relay nodes.

Step 3: Assume perfectly error-free DF relaying and the same transmit power at the relay as that of the source in the second EXIT chart, which examines the evolution of the input/output mutual information exchanges in the three-stage iterative decoder of the Ir-DST coding scheme. Use the EXIT curve matching algorithm of [12] to match the SNR-dependent EXIT curve of the amalgamated "STBC$_r$-IRCC$_r$" decoder to the target EXIT curve of the amalgamated "STBC$_s$-URC$_s$-IRCC$_s$" decoder observed in **Step 2**. Obtain the maximized average code rate R_r and the optimized weighting coefficients $\beta_j, j = 1,\ldots,17$ of IRCC$_r$ when a narrow-but-open EXIT-tunnel emerges.

In this contribution, we consider an average code rate of $R_s = 0.5$ for the outer IRCC$_s$ at the source node and the specific relay network configuration with $G_{sr} = 8$ and $G_{rd} = 2$, which satisfies Eq. (5). The EXIT chart of the serial concatenated IRCC$_s$-URC$_s$-STBC$_s$ scheme of the source-to-relay link is depicted in Fig. 5, where the decoding trajectories are computed based on a frame length of 250 000 bits. The EXIT curve of the outer IRCC$_s$ having optimized weighting coefficients α_i as shown in Fig. 5 was constructed using the curve matching algorithm of [12]. As we can see from Fig. 5, a narrow but marginally open EXIT tunnel emerges for the 2×2 source-to-relay communication link. A receive SNR of about -2.1 dB is needed in order to attain a decoding convergence to an infinitesimally low BER. Due to the geometrical-gain of the source-to-relay link, the equivalent SNR[5] at the source node can be computed as

$$\mathrm{SNR}_e^s = \mathrm{SNR}_r^{sr} - 10\log_{10}(G_{sr})[\mathrm{dB}] \ , \qquad (19)$$

where SNR_r^{sr} is the receive SNR at the relay node. Hence, the minimum SNR_e^s at the source node required for the sake of obtaining a near error-free performance at the relay node is -11.1 dB. As presented in Section II, we assume that both the source and relay transmit their signals at the same transmit power, hence they have the same equivalent SNR. In order to avoid the potentially high computational complexity at the relay node, a wider-than-necessary EXIT tunnel is created in the EXIT chart of Fig. 5 at the receive SNR of -1.0 dB at the relay node, which corresponds to an equivalent SNR of -10 dB based on Eq. (19) at both the source and relay nodes. As clearly seen in the EXIT chart of Fig. 6 at the destination node, after 5 "inner" iterations between the IRCC$_s$ decoder and the amalgamated "STBC$_s$-URC$_s$" decoder, the increase of the area A_E under the amalgamated "STBC$_s$-URC$_s$-IRCC$_s$" decoder becomes marginal. Hence, we fix the number of "inner" iterations to $I_i^d = 4$ at the destination node. Following the design procedure above, we obtain the resultant matching EXIT curve for the Ir-DST coding scheme in Fig. 6, where the IRCC$_r$ has the optimized weighting coefficients β_j and a maximized average code rate of $R_r = 0.5$, hence $L_s = L_r$. It is clearly seen in Fig. 6 that a narrow-but-open EXIT-tunnel emerges, which indicates the possibility of achieving decoding convergence to an infinitesimally low BER at near-capacity SNRs for the Ir-DST coding scheme. This prediction is verified in Fig. 6 by plotting the corresponding Monte-Carlo simulation-related decoding trajectory, which indeed reaches the (1.0,1.0) point of the EXIT chart. On the other hand, since the code rate R_r of the relay's IRCC has been maximized by the joint source-and-relay mode design procedure, the Ir-DST coding scheme achieves a maximum effective throughput of $\frac{L_s}{L_s+L_r} R_s \log_2 4 = 0.5$ bit/s/Hz, when the 4QAM-modulated G2 scheme is employed.

[5]Here we introduced the terminology of equivalent SNR$_e$ to define the ratio of the signal power at the transmitter side with respect to the noise level at the receiver side, i.e. $\mathrm{SNR}_e = P_0/N_0$, as in [14]. Although this does not have a direct physical interpretation, it simplifies our discussions.

V. Simulation Results and Discussions

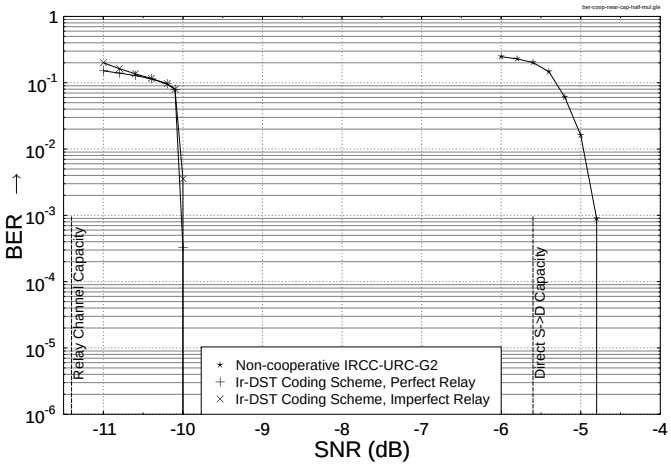

Fig. 7. BER versus equivalent SNR performance of both perfect and imperfect relaying Ir-DST and non-cooperative IRCC-URC-G2 schemes for a frame length of 250 000 bits, where the cooperative network is configured with $G_{sr} = 8$ and $G_{rd} = 2$ as well as $L_s = L_r$ and the non-cooperative system is equipped with two transmit and four receive antennas.

In this section, we present the BER versus equivalent SNR performance of both the perfect and imperfect relaying aided Ir-DST schemes as well as that of a non-cooperative serial concatenated IRCC-URC-STBC scheme in Fig. 7. For the Ir-DST coding scheme, according to the trajectory predictions seen in Figs. 5 and 6, the number of decoding iterations between the IRCC$_s$ decoder and the amalgamated "STBC$_s$-URC$_s$" decoder was fixed to $I^r = 13$ at the relay node. At the destination node, the number of "inner" decoding iterations was fixed to $I_i^d = 4$, while the number of "outer" decoding iterations between the parallel amalgamated "STBC$_s$-URC$_s$-IRCC$_s$" decoder and the amalgamated "STBC$_r$-IRCC$_r$" decoder was fixed to $I_o^d = 17$. On the other hand, for the non-cooperative IRCC-URC-STBC scheme, we employ an outer IRCC, which has the same weighting coefficients α_i and hence the same code rate as that of the IRCC$_s$ in the cooperative system. The number of decoding iterations exchanging extrinsic information between the outer IRCC decoder and the inner "STBC-URC" decoder was fixed to $I_{non} = 13$ as well.

As seen in Fig. 7, the Ir-DST coding scheme outperforms the non-cooperative IRCC-URC-STBC scheme by approximately 5.1 dB in terms of the required equivalent SNR, which corresponds to a 3 dB lower value of 2.1 dB in terms of E_b/N_0 due to a factor 0.5 multiplexing loss in the half-duplex Ir-DST scheme. On the other hand, the performance of the

perfect relaying-aided Ir-DST scheme matches the EXIT chart predictions of Fig. 6, while the imperfect relaying-aided Ir-DST coding scheme performs similarly to the perfect relaying scheme. This is due to the fact that the source information becomes near-error-free at the relay node after a sufficiently high number of decoding iterations. Furthermore, it is clearly shown in Fig. 7 that the Ir-DST coding scheme is capable of performing within 1.4 dB of the corresponding relay channel's DCMC capacity.

VI. Conclusions

In this contribution, we have proposed an Ir-DST coding scheme for near-capacity cooperative communications. We derived the CCMC capacity and the constrained information-rate bounds of Alamouti's G2 scheme for the half-duplex relay channel. The proposed joint source-and-relay mode design procedure is capable of finding the optimal Ir-DST coding scheme, which performs close to the capacity limit and achieves a maximum effective throughput. Furthermore, the code design procedure is not limited to a specific networking scenario, it is applicable under virtually any network configuration.

References

[1] A. Sendonaris, E. Erkip, and B. Aazhang, "User cooperation diversity: Part I and II," *IEEE Transactions on Communications*, vol. 51, pp. 1927–1948, Nov. 2003.

[2] J. Laneman, D. Tse, and G. Wornell, "Cooperative diversity in wireless networks: Efficient protocols and outage behavior," *IEEE Transactions on Information Theory*, vol. 50, pp. 3062–3080, Dec. 2004.

[3] J. Laneman and G. Wornell, "Distributed space-time-coded protocols for exploiting cooperative diversity in wireless networks," *IEEE Transactions on Information Theory*, vol. 49, pp. 2415–2425, Oct. 2003.

[4] K. Azarian, H. El Gamal, and P. Schniter, "On the achievable diversity-multiplexing tradeoff in half-duplex cooperative channels," *IEEE Transactions on Information Theory*, vol. 51, pp. 4152–4172, Dec. 2005.

[5] B. Zhao and M. Valenti, "Distributed turbo coded diversity for relay channel," *Electronics Letters*, vol. 39, pp. 786–787, May 2003.

[6] S. X. Ng, Y. Li and L. Hanzo, "Distributed turbo trellis coded modulation for cooperative communications," in *ICC'09*, (Dresden, Germany), 14-18 June 2009.

[7] S. ten Brink, "Convergence behaviour of iteratively decoded parallel concatenated codes," *IEEE Transactions on Communications*, vol. 49, pp. 1727–1737, Oct. 2001.

[8] S. ten Brink, "Designing iterative decoding schemes with the extrinsic information transfer chart," *AEU International Journal of Electronics and Communications*, vol. 54, pp. 389–398, Nov. 2000.

[9] Z. Zhang and T. Duman, "Capacity-approaching turbo coding for half-duplex relaying," *IEEE Transactions on Communications*, vol. 55, pp. 1895–1906, Oct. 2007.

[10] J. G. Proakis, *Digital Communications*. 4th ed. New York: McGraw-Hill, 2001.

[11] S. X. Ng and L. Hanzo, "On the MIMO channel capacity of multidimensional signal sets," *IEEE Transactions on Vehicular Technology*, vol. 55, pp. 528–536, March 2006.

[12] M. Tüchler and J. Hagenauer, "EXIT charts of irregular codes," in *Proceeding of the 36th Annual Conference on Information Sciences and Systems [CDROM]*, (Princeton, NJ, USA), March 2002.

[13] M. Tüchler, "Design of serially concatenated systems depending on the block length," *IEEE Transactions on Communications*, vol. 52, pp. 209–218, Feb. 2004.

[14] H. Ochiai, P. Mitran and V. Tarokh, "Design and analysis of collaborative diversity protocols for wireless sensor networks," in *VTC'04 Fall*, (Los Angeles, CA), pp. 4645–4649, 26-29 Sept. 2004.

[15] A. Host-Madsen and J. Zhang, "Capacity bounds and power allocation for wireless relay channels," *IEEE Transactions on Information Theory*, vol. 51, pp. 2020–2040, June 2005.

[16] A. Host-Madsen, "Capacity bounds for cooperative diversity," *IEEE Transactions on Information Theory*, vol. 52, pp. 1522–1544, April 2006.

[17] S. M. Alamouti, "A simple transmit diversity technique for wireless communications," *IEEE Journal on Selected Areas in Communications*, vol. 16, pp. 1451–1458, Oct. 1998.

[18] D. Divsalar, S. Dolinar and F. Pollara, "Serial turbo trellis coded modulation with rate-1 inner code," in *ISIT*, (Sorrento, Italy), p. 194, 25-30 June 2000.

[19] L. Hanzo, T. H. Liew and B. L. Yeap, *Turbo Coding, Turbo Equalisation and Space Time Coding for Transmission over Wireless channels*. New York, USA: John Wiley IEEE Press, 2002.

[20] T. M. Cover and A. E. Gamal, "Capacity theorems for the relay channel," *IEEE Transactions on Information Theory*, vol. 25, pp. 572–584, Sept. 1979.

[21] S. X. Ng and S. Das and J. Wang and L. Hanzo, "Near-Capacity Iteratively Decoded Space-Time Block Coding," in *IEEE VTC'08 (Spring)*, (Marina Bay, Singapore), pp. 590–594, 11-14 May 2008.

[22] S. X. Ng, J. Wang and L. Hanzo, "Unveiling Near-Capacity Code Design: The Realization of Shannon's Communication Theory for MIMO Channels," in *ICC'08*, (Beijing, China), pp. 1415–1419, 19-23 May 2008.

[23] L. Kong, S. X. Ng and L. Hanzo, "Near-capacity three-stage downlink iteratively decoded generalized layered space-time coding with low complexity," in *GLOBECOM'08*, (New Orleans, LA, USA), pp. 1–6, 30 Nov.-04 Dec. 2008.